HHS Public Access

Author manuscript

Bone. Author manuscript; available in PMC 2015 September 22.

Published in final edited form as:

Bone. 2013 February ; 52(2): 644–650. doi:10.1016/j.bone.2012.10.032.

Contributions of Severe Burn and Disuse to Bone Structure and Strength in Rats

L.A. Baer[a,b], **X. Wu**[a,d], **J. C. Tou**[c], **E. Johnson**[d], **S.E. Wolf**[a,e], and **C.E. Wade**[a,b]

[a]US Army Institute of Surgical Research, 3611 Rawley E Chambers, Fort Sam Houston, TX 78234

[b]The University of Texas Health Science Center at Houston, Department of Surgery and Center for Translational Injury Research, 6431 Fannin St, MSB 5.214, Houston, TX 77030

[c]West Virginia University, Animal and Nutritional Sciences, PO Box 6201, Morgantown, WV, 26506

[d]M.D. Anderson Small Animal Imaging Facility, 1515 Holcombe Blvd, Houston, TX 77030

[e]The University of Texas Southwestern Medical Center, Department of Surgery, 5323 Harry Hine Blvd, Dallas, TX 75390

Abstract

Burn and disuse results in metabolic and bone changes associated with substantial and sustained bone loss. Such loss can lead to an increased fracture incidence and osteopenia. We studied the independent effects of burn and disuse on bone morphology, composition and strength, and microstructure of the bone alterations 14 days after injury. Sprague-Dawley rats were randomized into four groups: Sham/Ambulatory (SA), Burn/Ambulatory (BA), Sham/Hindlimb Unloaded (SH) and Burn/Hindlimb Unloaded (BH). Burn groups received a 40% total body surface area full-thickness scald burn. Disuse by hindlimb unloading was initiated immediately following injury. Bone turnover was determined in plasma and urine. Femur biomechanical parameters were measured by three-point bending tests and bone microarchitecture was determined by microcomputed tomography (uCT). On day 14, a significant reduction in body mass was observed as a result of burn, disuse and a combination of both. In terms of bone health, disuse alone and in combination affected femur weight, length and bone mineral content. Bending failure energy, an index of femur strength, was significantly reduced in all groups and maximum bending stress was lower when burn and disuse were combined. Osteocalcin was reduced in BA compared to the other groups, indicating influence of burn. The reductions observed in femur weight, BMC, biomechanical parameters and indices of bone formation are primarily responses to the

Corresponding Author: Lisa A. Baer, University of Texas Health Science Center at Houston, 6431 Fannin St, MSB 5.214, Houston, TX 77030, Phone: (713)500-7447, Fax: (713)500-0685, lisa.baer@uth.tmc.edu.

Disclosures

No conflicts of interest, financial or otherwise, are declared by the authors.

combination of burn and disuse. These results offer insight into bone degradation following severe injury and disuse.

Keywords

hindlimb unloading; thermal injury; femur; mechanical bending; micro-computed tomography

1. Introduction

Burn injuries of ≥40% total body surface area (TBSA) has markedly reduced bone formation in both adults and children [1]. Burn induces a systemic catabolic response characterized by increased energy expenditure [2–4]. This increased expenditure produces a rapid and severe depletion of body energy stores, which are associated with a loss of bone calcium and subsequently osteopenia [5, 6]. In addition, it is suggested that bone loss begins in the first 24 hours following injury due to a rise in proinflammatory cytokines and the surge of glucocorticoids over the first week. Both of these responses are directly linked to an increase in osteoclastogenesis resulting in bone resorption [7]. Reduced skeletal loading (i.e. bed rest) following any type of injury can also be a significant contributing factor to loss of bone density and strength [8]. Bed rest causes an uncoupling of resorption and formation in the remodeling of bone, which tends to favor resorption, rather than formation. Remodeling is a surface event, therefore, a larger surface area has a greater susceptibility to bone loss than those with less surface area bone [9–11]. Thus, it is expected that bone loss due to disuse would tend to be more severe in trabecular bone than cortical bone because the trabecular bone has 4X greater surface area than cortical bone [12]. Both bone mass and architecture are key components which influence the mechanical properties of bone [13].

Bed rest after burn injury is a contributing factor to the overall outcome of the patients' health and well-being. Following seven days of bed rest, adult patients with greater than 50% TBSA burn have lower bone formation rates than patients without burns [1, 14]. Reductions in bone growth and changes in bone remodeling can have long-lasting adverse consequences for patients during rehabilitation. Decreased bone mineral content (BMC), which occurs within eight weeks of injury, may last up to five years due to the reduction in bone formation [3, 5, 15] and thus may be associated with a higher incidence of fractures and osteoporosis [3, 16, 17]. Using two and three-dimensional imaging techniques, such as micro-computed tomography (μCT), allows for complete information on the microarchitecture of the bone [13].

Animal models have been used to study the physiological effects of severe burn or disuse separately [18–22]. Previous animal burn models are able to replicate the hypermetabolic and insulin resistant effects of the injury, however, not the musculoskeletal effects from disuse. We developed a clinically relevant animal model that reproduces the physiological and metabolic, as well as the musculoskeletal responses of a burn patient immediately transferred into bed rest [21]. In the current study, our clinically relevant animal model of burn and disuse, both as independent components and in combination, was used to investigate the effects on bone morphometry, turnover, mass, strength and microachitecture. Understanding bone structure and microstructure and how it is affected by both burn injury

and disuse is important in determining possible therapeutic approaches for improved long term quality of life.

2. Material and Methods

All procedures were approved by the US Army Institute of Surgical Research Institutional Animal Care and Use Committee and conducted in accordance with the Guide for Care and Use of Laboratory Animals [23].

2.1 Animals and Housing

Male, Sprague-Dawley rats were used for this study (Charles Rivers, Wilmington, MA). Animals were approximately 300g at the start of the experiment. Upon arrival, animals were housed in standard vivarium cages and then moved into specialized hindlimb unloading/metabolic (HLU) cages (144 in^2 usable floor area) six days before injury to allow for acclimation [24]. Animals were fed a certified diet (Harlan Teklad #2018) in powder-form while housed in the HLU cages. Food and water were available *ad libitum* throughout the study. The room light cycle was set at 12:12 hr (0600 on: 1800 off). Room temperature was maintained at 26±2 °C, with a relative humidity of 30–80% to simulate, as closely as possible, the ambient temperature maintained in a standard burn unit.

2.2 Experimental Group Assignments

Rats were assigned to one of four experimental groups: Sham/Ambulatory (SA; n=10); Burn/Ambulatory (BA; n=9); Sham/Hindlimb Unloading (SH; n=10); Burn/Hindlimb Unloading (BH; n=10). A block design was used for this study where four animals were weight-matched to each other and then each animal was randomly assigned to one of the four treatment groups. This assignment was carried out prior to any experimental manipulations.

2.3 Scald Injury

Rats randomly assigned to either burn treatment group (i.e. BA or BH) received a 40% total body surface area, full-thickness scald burn as described by Walker-Mason [25]. Rats were anesthetized with isoflurane (2–3% in 100% O_2) throughout the procedure and administered buprenorphine (0.05 mg/kg s.c) prior to injury. Each rat was shaved and secured in a plexiglass mold exposing 20% of the total body surface area of the dorsal side. The dorsal surface was submerged in 100°C water for 10 seconds. The animal was removed from the mold, administered 20cc of Lactated Ringer's intraperitoneally, which was based on the Parkland Formula for resuscitation fluids in burn patients [26], placed back in the mold exposing the ventral (belly) surface and submerged in 100°C water for two seconds. Sham groups (SA and SH) were exposed to the anesthesia procedure, shaved and submerged in water at room temperature. All animals were administered additional analgesics (buprenorphine; 0.05 mg/kg s.c) 6–8 hours following the scald procedure for 72 hours.

2.4 Hindlimb Unloading

Following the scald procedure described above, animals were randomly assigned to the HLU group were placed in a tail traction system using an established HLU model [24].

Briefly, the tail was prepared for HLU by cleaning with alcohol wipes, tincture of benzoin was then applied, allowing it to become tacky to the touch. A ½″ strip of Skin Trac© (Zimmer, San Jose, CA) was secured on the tail, it was then wrapped in Stockinette, and 3-1″ strips of filament fiber tape were applied (base, middle, top). Animals were allowed to completely recover from anesthesia, approximately 20–30 min, before being placed in HLU cages and their hind limbs were unloaded approximately 30° using a hook and pulley system. The pulley system allowed the animals to have 360° access within the cage environment without applying load to their hind limbs. Animals were observed immediately after unloading for any apparent signs of distress and were monitored several times during the day throughout the study following the burn/HLU procedure.

Body mass of all animals were measured daily from the time of arrival until the end of the study. Animals assigned to SH and BH treatment groups were weighed using a hook attached to a ring-stand placed on the balance to avoid any type of weight-bearing on the hindlimbs during the weighing procedure [24]. Food and water intake were measured daily on all groups.

2.5 Urine collection

Housing in the HLU cages allowed for the collection of uncontaminated urine samples. Beginning one day before burn/hindlimb unloading (baseline), 24-hour urine measurements were taken. Mineral oil (0.5 mL) was added to each urine collection tube to avoid any potential evaporation of the collected urine over the 24-hour period. This amount was accounted for at the time the urine volume was measured. Urine was aliquoted and analyzed for total urinary calcium (Ca^{++}) and phosphorus (P) and bone turnover markers.

2.6 Bone Turnover Marker Measurements

Plasma osteocalcin (bone gamma-carboxyglutamic acid peptide), an indicator of osteoblastic activity and bone formation, was determined by a commercial enzyme-linked-immunosorbent assay (ELISA) (Immunodiagnostic Systems, Fountain Hills, AZ). Urinary deoxypyridinoline (DPD), an indicator of osteoclast activity and bone resorption and degradation, was measured by commercial urinary ELISA (Quidel Corp, San Diego, CA) using a 15-day (Baseline+ 14 experimental days) pooled sample of 0.01% of the total urine volume for each experimental day.

At the conclusion of the 14-day study, animals were deeply anesthetized with isoflurane (1–3% in 100% O_2), blood was collected via cardiac puncture and the animals were euthanized by exsanguination. Blood was transferred to heparinized vacutainers and kept on ice until processing. Whole blood was centrifuged at 4°C, for 15 minutes at 3000 RPM. Plasma was collected and stored at −80°C until analysis. Femurs were removed, cleaned of any extraneous muscle, wrapped in saline-soaked gauze and stored at −20°C until further processing.

2.7 Micro-CT Imaging

Contralateral femurs were imaged at the University of Texas M.D. Anderson Small Animal Imaging Facility (SAIF) in a Locus SP micro-CT unit (GE Medical Systems, London, ON).

Each bone was wrapped in saline-soaked gauze and placed in a specimen holder along with a small 2 mL vial of water and a hydroxyapatite phantom to ensure CT value Hounsfeld Units consistency. Each bone was imaged at 80 kVp, 80 μA, and at a resolution level producing isotropic 25-μm voxel data. The scans consisted of 500 projection views at 0.72 degree increments, with each view having a total exposure time of 12 seconds (4 averaged frames at 3 seconds exposure each). Following the scan and subsequent correction process, each data set was processed as 3 reconstructions per bone: a 25-μm voxel midshaft region (approximately 5 mm^3), a 25-μm voxel distal region (7 mm in length, extending from the growth plate), and a 50-μm voxel reconstruction of the entire femur. For the full femur, bone volume, BMC, bone mineral density (BMD), tissue mineral content, tissue mineral density and bone volume fraction were determined. For the trabecular regions of the distal femur, bone volume fraction, bone surface to volume ratio, trabecular thickness, trabecular separation and trabecular number were determined. For the midshaft region of the cortical bone, mean thickness, inner perimeter, outer perimeter, marrow area, cortical area, total area, BMD and BMC were measured.

2.8 Femur Biomechanics

Femur bone strength parameters were assessed on using a TA.HDi Texture Analyzer (Texture Technologies Corp, New York, NY) outfitted with a three-point bending apparatus. Femurs were placed on supports (1 mm width at tip) and force was applied to the mid-shaft halfway between the greater trochanter and the distal medial condyle until broken by lowering a centrally placed blade (1 mm width) at constant crosshead speed (0.1 mm/s). The load cell was 250 kg. The load-deflection data collected by a computer interfaced with the TA.HDi Texture Analyzer was used to determine bone biomechanical measurements, described as the following [27]:

1. *Peak force (N)*: the maximum force obtained during the bending procedure resulting in the initiation of bone failure which is propagated to the point where the bone breaks and the force reading drops to zero.
2. *Bending failure energy (-N*s)*: the work energy (area under the time-force deformation curve) required to achieve failure of the bone in bending.
3. *Ultimate Stiffness (N/mm)*: the slope of the time-force deformation curve.
4. *Ultimate bending stress (N/mm^2)*: a normalized, calculated force value that takes into consideration bone size.
5. *Young's Modulus* (*N/mm^2*): a measure of the stiffness of an isotrophic elastic material.

2.9 Mineral Determination

Total plasma and urinary Ca^{++} and P were determined using the Dade Dimension Chemistry Analyzer® (Deerfield, IL). Femur Ca^{++}, P and BMC were determined by established ashing procedures as described previously [28]. Following biomechanical testing, bone fragments were dried at 110°C for 48h. Dried bones were ashed by placing in a muffle furnace at 600°C for 24h. Total BMC was determined by weighing the ashed sample. To measure bone

Ca^{++} and P, samples were dissolved in 2 mL of 70% nitric acid. The acidified samples were neutralized in 5 mL of deionized distilled water (ddH2O) and filtered through Whatman paper. Samples were then diluted to a final volume of 500 mL with ddH2O. Femur Ca^{++} and P were measured using an inductively coupled plasma mass spectrometry (model P400 Perkin Elmer, Shelton, CT).

2.10 Statistics

SigmaPlot (Windows ver.11.0, Systat Software, Inc., San Jose, CA) was used to perform the statistical analysis. A one-way analysis of variance (ANOVA) between treatments was performed. The Student Neuman-Keuls *post hoc* analysis was performed when applicable. Linear relationships were determined using the Pearson Product Moment correlation. Values are expressed as mean ± standard error of the mean (SEM) and p values <0.05 were considered statistically significant.

3. Results

3.1 Body mass

There were no differences in initial body mass between treatment groups, however, differences were apparent by day 14 (Table 1). BA and SH showed similar reductions in body mass and BH had the most dramatic decrease over time, accentuated by an additive effect from the combination of burn and disuse. (Table 1). Percent body mass decrease over time was the greatest in BH rats at day 14 ($p<0.001$; Figure 1).

3.2 Bone morphology

As compared to SA, both SH and BH had significantly lower femur weights ($p<0.02$). BA was different from SA, and both HLU groups (SH & BH), irrespective of burn, showed a significant difference from SA. This suggests that disuse had a greater influence on femur weight than the burn component (Table 1). Total BMC determined in ashed femurs was significantly reduced in BA, SH and BH compared to SA ($p<0.001$; Table 1). However, BA, SH and BH ashed femur BMC were not different from each other. A strong, positive association was observed between femur weight and ashed femur BMC ($r=0.72$, $p<0.001$, $n=39$; Figure 2), suggesting BMC may be a contributing factor to the differences in bone weight.

Femur morphology, including length, diameter and width, was also determined. Compared to SA, a significant decrease in femur length was observed in the BH group only ($p<0.001$). No significant differences were observed with femur width or diameter in any group (Table 1).

Bone composition has a direct influence on bone strength, as there is a moderate positive association between bending failure energy and ashed femur BMC ($r=0.55$, $p<0.0003$, $n=39$) (Figure 3a). This association suggests that relative reduction in mineral content contributes to the time to failure. A positive association was observed between ultimate bending stress and ashed femur BMC ($r=0.47$, $p<0.0003$, $n=39$; Figure 3b).

3.3 Bone turnover analyses

Plasma osteocalcin, a marker for bone formation, was significantly reduced in BA as compared to all other treatment groups ($p<0.005$). There was no significant difference between the other groups, as the effect of burn appears to be negated by disuse because even though burn had an effect on osteocalcin concentration, osteocalcin concentration in BH was similar to those in SA (Figure 4). Also, there may be other underlying mechanisms involved that may account for these changes. Urinary DPD, an indication of bone resorption and degradation, was measured in pooled urine samples. No differences in total urinary DPD were observed between any of the groups for the duration of the study. In addition, no differences were observed when corrected for renal function indicated by DPD to creatinine ratio (DPD/creatinine [nmol/mmol]: SA=227.6±12.2; BA=217.5±12.4; SH=194.9±16.9; BH=235.5±30.5; NS). No differences in Ca^{++} or P levels were observed between any of the treatment groups (Table 3).

3.4 Bone biomechanical strength

Measurements in femur strength were peak force, bending failure energy, ultimate stiffness, ultimate bending stress and Young's modulus. Bending failure energy was lower in all groups compared to SA ($p<0.001$), but no differences were observed between SH, BA and BH; both burn and disuse had a similar overall and independent effect on bone outcome which was not additive in this parameter. Ultimate bending stress, which takes the overall bone size into consideration, was significantly reduced in the BH group as compared to the other groups ($p<0.001$). The shortening of the bone may have a direct influence on this measurement. Young's modulus, which is defined as the uniaxial stress over the uniaxial strain, was significantly lower in the BH group as compared to SA and SH ($p<0.05$); however, there were no significant differences between BH and BA, suggesting that this measurement is affected primarily by the burn component (Table 2).

3.5 Bone microarchitecture

Using μCT, the effects of burn and disuse, both as independent contributors and combined, were evident in the full bone, as well as trabecular and distal regions (Fig 5a–d; Table 4). The total volume of the region of interest demonstrated an additive effect as BH was significantly reduced ($p<0.03$) when calculated as a percent of SA (84%), BA (92%) and SH (90%). No differences were observed between BA and SH. The response of burn and disuse independently showed similar effects between treatments. BMC measured by μCT was significantly reduced from SA in the BA and BH ($p<0.001$) groups, as was total mineral content in BA and BH ($p<0.001$). There was a positive association observed between ashed BMC and the μCT BMC output ($r=0.62$; $p<0.001$; $n=39$) validating the two measurements. There was no effect on BMD, tissue mineral density or bone volume fraction. The effect of the combination of burn and disuse was more prominent in the cortical bone than the trabecular bone. In the distal trabecular bone, even though there was a significant decrease in total volume in BH as compared to SA ($p<0.04$), the majority of the indices measured were primarily affected by disuse alone compared to the other treatment groups. Bone fraction volume to total volume was significantly decreased in SH as compared to SA ($p<0.02$), while bone surface to bone volume ratio was significantly increased in SH as

compared to SA ($p<0.02$), but decreased in BA and BH ($p<0.001$). BMD was significantly decreased in SH as compared to the SA ($p<0.03$), but increased as compared to BA ($p<0.008$). There were no differences in trabecular separation or tissue mineral density. In the midshaft cortical bone, mean thickness and cortical area were significantly reduced in BA ($p<0.03$) and BH ($p<0.01$) as compared to SA ($p<0.01$). No other differences were observed (Table 4).

The effect of the combination of burn and disuse was more prominent in the cortical bone than the trabecular bone. In the trabecular bone, even though we found a significant increase in total volume in BH as compared to SA ($p<0.04$), the majority of the indices measured were primarily affected by disuse alone compared to the other treatment groups.

4. Discussion

Previous studies have shown that severe burn and disuse, as a result of bed rest following injury, dramatically affect the physiological and endocrine systems of patients [21, 29]. These injuries lead to an immediate change in metabolism including a period of hypermetabolism and catabolism. Coupled with these changes, it is suggested that bone loss begins in the first 24 hours following injury, due to the rise in proinflammatory cytokines and then a surge of glucocorticoids that continues over the first week as a result of the injury. Both of these responses, are directly linked to an increase in osteoclastogenesis resulting in bone resorption [7]. In this and follow-up studies we did observe an immediate rise in proinflammatory cytokines and corticosterone of approximately 5 times that of controls when burn and disuse were combined (Baer, unpublished data). One main complication of severe burn is the loss of bone during bed rest, resulting in potential issues following discharge, including increased incidence of fractures and osteopenia. Reduced bone lengths and weights have been documented in children with burns and have been attributed to the extended bed rest and severity of burn altering skeletal formation [6], which we also determined in our rat model of burn and disuse. However, the specific contributions of burn and disuse causing these alterations in bone morphology, composition and strength have yet to be studied in great detail results. Our rat model, like a burn patient, does allow for movement of their hind limbs, however they are in a non-weight bearing state. This does not reflect a true immobilized state, supporting that the changes in muscle and bone are a reflection of the state that they are in.

Historically, the rat is a useful model to examine the muscular and skeletal changes that occur due to thermal injury [14, 21, 30, 31]. In the present study, we demonstrated changes in body mass, bone composition and bone mechanical properties with the use of separate established burn and disuse models that were amplified when combined. Mechanical bone properties, including breaking and mechanical strength are shown to be negatively affected by burn and disuse. Our model illustrated that femur mechanical strength, as well as bone length, bone weight and ashed femur BMC are reduced.

The observation of a reduction in breaking strength, lead us to look at possible mechanisms that contribute to bone weakness. Urinary and plasma calcium and phosphorus have been shown to have a direct correlation to the composition of bone [32]. In the burn groups, we

found urinary excretion of calcium tended to be increased, however not significantly. Calcium intake was not different between groups; therefore we can conclude the absorption of calcium is not a contributing factor to the alteration of bone properties. Calcium has an established, direct relationship with bone strength, and the reduction in the present model elicited may suggest an explanation for changes in breaking strength.

Patients who experienced a burn greater than 30% TBSA show a decrease in osteocalcin possibly attributing to a reduction in bone formation. This outcome has been postulated to contribute to the increase in fracture rates in both children and adult patients following burns [3, 16, 33, 34], despite data showing no changes in osteocalcin levels in patients with less than 25% TBSA [35]. Previous studies in hindlimb unloaded rats of the same time course show, as in the present study, plasma osteocalcin levels initially decrease, but return to baseline concentrations by day 14 [36, 37]. In our study, 40% TBSA burn alone resulted in a reduction in plasma osteocalcin concentrations at day 14, however when the disuse component was introduced in the combined model, the reduction was negated. The osteocalcin response in rats is more acute compared to that of humans in bedrest studies, which may signify a possible species difference. We feel there may be additional mechanisms involved once disuse is introduced that require further investigation.

Metabolically, a well-defined endocrine response occurs after burn injury, affecting several hormones not only by the initial injury, but also during the recovery period [38]. Urinary DPD, used as a marker of bone resorption, has been shown to be increased in humans during bed rest and with burns [35, 39–41]. In the animal model of burn and disuse, pooled DPD was found not to be changed among the treatment groups, possibly suggesting other mechanisms may be overwhelming the endocrine system. The inability to detect sizable changes may be masked by using a pooled sample, however we feel that any changes would occur early and still would be apparent in a pooled sample. To assure possible detection in future studies, measurements on each corresponding day should be considered.

The use of μCT is an additional tool to determine associations between bone strength, bone resorption and formation. We found disuse not only to be a contributing factor, but the burn injury caused an additive component. The combination injury results in many changes that are reflected more in the full and trabecular bone rather than cortical bone. The components affecting the full bone, including bone volume, BMC and TMC are a direct influence on bone strength outcome. Trabecular bone, which has approximately four times greater surface area as cortical bone, shows significant remodeling occurring in the combined burn and disuse as well as the burn group. This is evidenced by bone surface density (BS/BV). Meanwhile cortical bone in limited indices, was more directly affected by the burn injury. As compared to controls, changes irrespective of treatment group in the full bone, as well as cortical and trabecular, suggest significant alterations occur following this type of severe injury.

By using our clinically relevant animal model for severe burn and disuse, we were able to demonstrate that the combination of severe burn and disuse elicits similar metabolic patterns as observed in victims of severe burns and elucidates underlying factors contributing to overall physiological changes in bone. However, as with any animal model, there will

always be certain limitations as compared to the clinical environment. By applying a clinically relevant animal model, which is able to simulate bone metabolism changes similar to those in patients, therapies assisting with either the prevention, or possible rehabilitative activities, can be calculated during the period of disuse following injury. These interventions can help with problems in bone health that have been identified in the burn patient population following discharge.

Acknowledgments

The authors would like to thank Angela Beeler and R. Michelle Sauer, Ph.D for their editorial support.

Grants

This research was funded by the National Institutes of Health (1 R01 GM063120-04), the Technologies for Metabolic Monitoring (TMM)/Julia Weaver Fund, A Congressionally Directed Program Jointly Managed by the USA MRMC, NIH, NASA and the Juvenile Diabetes Research Foundation And Combat Casualty Care Division United States Army Medical Research and Materiel Command. The funding sources had no involvement in the study design, data collection, analysis, interpretation of the data, writing this manuscript or the decision to submit this article for publication.

Glossary

BA	Burn/Ambulatory
BH	Burn/Hindlimb Unloaded
BMC	bone mineral content
DPD	deoxypyridinoline
ELISA	enzyme-linked immunosorbent assay
HLU	hindlimb unloading
SA	Sham/Ambulatory
SEM	standard error of the mean
SH	Sham/Hindlimb Unloaded
TBSA	total body surface area
uCT	micro-computed tomography

References

1. Klein GL, Herndon DN, Rutan TC, Sherrard DJ, Coburn JW, Langman CB, Thomas ML, Haddad JG Jr, Cooper CW, Miller NL, et al. Bone disease in burn patients. J Bone Miner Res. 1993; 8:337–45. [PubMed: 8456588]
2. Hart DW, Wolf SE, Chinkes DL, Gore DC, Mlcak RP, Beauford RB, Obeng MK, Lal S, Gold WF, Wolfe RR, Herndon DN. Determinants of skeletal muscle catabolism after severe burn. Ann Surg. 2000; 232:455–65. [PubMed: 10998644]
3. Klein GL, Herndon DN, Langman CB, Rutan TC, Young WE, Pembleton G, Nusynowitz M, Barnett JL, Broemeling LD, Sailer DE, et al. Long-term reduction in bone mass after severe burn injury in children. J Pediatr. 1995; 126:252–6. [PubMed: 7844672]

4. Klein GL, Herndon DN, Rutan TC, Miller NL, Alfrey AC. Elevated serum aluminum levels in severely burned patients who are receiving large quantities of albumin. J Burn Care Rehabil. 1990; 11:526–30. [PubMed: 2286606]
5. Demling RH, Seigne P. Metabolic management of patients with severe burns. World J Surg. 2000; 24:673–80. [PubMed: 10773119]
6. Shea JE, Bowman BM, Miller SC. Alterations in skeletal and mineral metabolism following thermal injuries. J Musculoskelet Neuronal Interact. 2003; 3:214–22. [PubMed: 15758344]
7. Klein GL. Burn-induced bone loss: importance, mechanisms, and management. J Burns Wounds. 2006; 5:e5. [PubMed: 16921418]
8. Rutan RL, Herndon DN. Growth delay in postburn pediatric patients. Arch Surg. 1990; 125:392–5. [PubMed: 2306187]
9. Bloomfield SA, Hogan HA, Delp MD. Decreases in bone blood flow and bone material properties in aging Fischer-344 rats. Clin Orthop Relat Res. 2002:248–57. [PubMed: 11859250]
10. Hefferan TE, Evans GL, Lotinun S, Zhang M, Morey-Holton E, Turner RT. Effect of gender on bone turnover in adult rats during simulated weightlessness. J Appl Physiol. 2003; 95:1775–80. [PubMed: 12882994]
11. Squire M, Brazin A, Keng Y, Judex S. Baseline bone morphometry and cellular activity modulate the degree of bone loss in the appendicular skeleton during disuse. Bone. 2008; 42:341–9. [PubMed: 17997144]
12. Foldes J, Parfitt AM, Shih MS, Rao DS, Kleerekoper M. Structural and geometric changes in iliac bone: relationship to normal aging and osteoporosis. J Bone Miner Res. 1991; 6:759–66. [PubMed: 1950680]
13. Laib A, Barou O, Vico L, Lafage-Proust MH, Alexandre C, Rugsegger P. 3D micro-computed tomography of trabecular and cortical bone architecture with application to a rat model of immobilisation osteoporosis. Med Biol Eng Comput. 2000; 38:326–32. [PubMed: 10912350]
14. Fang CH, Li BG, Tiao G, Wang JJ, Fischer JE, Hasselgren PO. The molecular regulation of protein breakdown following burn injury is different in fast- and slow-twitch skeletal muscle. Int J Mol Med. 1998; 1:163–9. [PubMed: 9852215]
15. Edelman LS, McNaught T, Chan GM, Morris SE. Sustained bone mineral density changes after burn injury. J Surg Res. 2003; 114:172–8. [PubMed: 14559443]
16. Klein GL, Herndon DN, Goodman WG, Langman CB, Phillips WA, Dickson IR, Eastell R, Naylor KE, Maloney NA, Desai M, et al. Histomorphometric and biochemical characterization of bone following acute severe burns in children. Bone. 1995; 17:455–60. [PubMed: 8579956]
17. Klein GL, Kikuchi Y, Sherrard DJ, Simmons DJ, Biondo N, Traber DL. Burn-associated bone disease in sheep: roles of immobilization and endogenous corticosteroids. J Burn Care Rehabil. 1996; 17:518–21. [PubMed: 8951538]
18. Hilder TL, Baer LA, Fuller PM, Fuller CA, Grindeland RE, Wade CE, Graves LM. Insulin-independent pathways mediating glucose uptake in hindlimb-suspended skeletal muscle. J Appl Physiol. 2005; 99:2181–8. [PubMed: 16099889]
19. Jeschke MG, Herndon DN, Finnerty CC, Bolder U, Thompson JC, Mueller U, Wolf SE, Przkora R. The effect of growth hormone on gut mucosal homeostasis and cellular mediators after severe trauma. J Surg Res. 2005; 127:183–9. [PubMed: 16083754]
20. Stein TP, Wade CE. Metabolic consequences of muscle disuse atrophy. J Nutr. 2005; 135:1824S–1828S. [PubMed: 15987873]
21. Wu X, Baer LA, Wolf SE, Wade CE, Walters TJ. The Impact of Muscle Disuse on Muscle Atrophy in Severely Burned Rats. Journal of Surgical Research. 2010; 164:e243–e251. [PubMed: 20888588]
22. Wu XW, Spies M, Chappell VL, Herndon DN, Thompson JC, Wolf SE. Effect of bombesin on gut mucosal impairment after severe burn. Shock. 2002; 18:518–22. [PubMed: 12462559]
23. Council NR. Guide for the care and use of laboratory animals. 8. Washington, DC: National Academy of Sciences; 2011.
24. Morey-Holton ER, Globus RK. Hindlimb unloading rodent model: technical aspects. J Appl Physiol. 2002; 92:1367–77. [PubMed: 11895999]

25. Walker HL, Mason AD Jr. A standard animal burn. J Trauma. 1968; 8:1049–51. [PubMed: 5722120]
26. Blumetti J, Hunt JL, Arnoldo BD, Parks JK, Purdue GF. The Parkland formula under fire: is the criticism justified? J Burn Care Res. 2008; 29:180–6. [PubMed: 18182919]
27. Yuan YV, Kitts DD. Dietary (n-3) fat and cholesterol alter tissue antioxidant enzymes and susceptibility to oxidation in SHR and WKY rats. J Nutr. 2003; 133:679–88. [PubMed: 12612137]
28. Tsanzi E, Fitch CW, Tou JC. Effect of consuming different caloric sweeteners on bone health and possible mechanisms. Nutr Rev. 2008; 66:301–9. [PubMed: 18522618]
29. Shangraw RE, Jahoor F, Miyoshi H, Neff WA, Stuart CA, Herndon DN, Wolfe RR. Differentiation between septic and postburn insulin resistance. Metabolism. 1989; 38:983–9. [PubMed: 2677612]
30. Jeschke MG, Klein D, Thasler WE, Bolder U, Schlitt HJ, Jauch KW, Weiss TS. Insulin decreases inflammatory signal transcription factor expression in primary human liver cells after LPS challenge. Mol Med. 2008; 14:11–9. [PubMed: 18037968]
31. Schaffler MB, Li XJ, Jee WS, Ho SW, Stern PJ. Skeletal tissue responses to thermal injury: an experimental study. Bone. 1988; 9:397–406. [PubMed: 3248203]
32. Creedon A, Cashman KD. The effect of calcium intake on bone composition and bone resorption in the young growing rat. Br J Nutr. 2001; 86:453–9. [PubMed: 11591232]
33. Delmas PD. What do we know about biochemical bone markers? Baillieres Clin Obstet Gynaecol. 1991; 5:817–30. [PubMed: 1822819]
34. Garnero P, Delmas PD. New developments in biochemical markers for osteoporosis. Calcif Tissue Int. 1996; 59 (Suppl 1):S2–9. [PubMed: 8974724]
35. Leblebici B, Sezgin N, Ulusan SN, Tarim AM, Akman MN, Haberal MA. Bone loss during the acute stage following burn injury. J Burn Care Res. 2008; 29:763–7. [PubMed: 18695620]
36. Buckendahl AC, Budczies J, Fiehn O, Darb-Esfahani S, Kind T, Noske A, Weichert W, Sehouli J, Braicu E, Dietel M, Denkert C. Prognostic impact of AMP-activated protein kinase expression in ovarian carcinoma: Correlation of protein expression and GC/TOF-MS-based metabolomics. Oncol Rep. 2011
37. Zhai L, Messina JL. Age and tissue specific differences in the development of acute insulin resistance following injury. J Endocrinol. 2009; 203:365–74. [PubMed: 19752148]
38. Dolecek R. Endocrine changes after burn trauma--a review. Keio J Med. 1989; 38:262–76. [PubMed: 2511373]
39. Akcay MN, Akcay G, Yilmaz I. The effect of calcitonin and growth hormone on urinary deoxypyridinoline levels in burned patients. Burns. 2002; 28:311–3. [PubMed: 12052368]
40. Kim H, Iwasaki K, Miyake T, Shiozawa T, Nozaki S, Yajima K. Changes in bone turnover markers during 14-day 6 degrees head-down bed rest. J Bone Miner Metab. 2003; 21:311–5. [PubMed: 12928833]
41. Smith SM, Nillen JL, Leblanc A, Lipton A, Demers LM, Lane HW, Leach CS. Collagen cross-link excretion during space flight and bed rest. J Clin Endocrinol Metab. 1998; 83:3584–91. [PubMed: 9768669]

Highlights

- Evaluated the use of clinically relevant animal model of severe burn injury and disuse
- The combination of burn injury and disuse has an additive effect.
- Bone morphological parameters are reduced by burn injury and disuse, independent and in combination.
- Burn and disuse was associated with reduced bone strength.

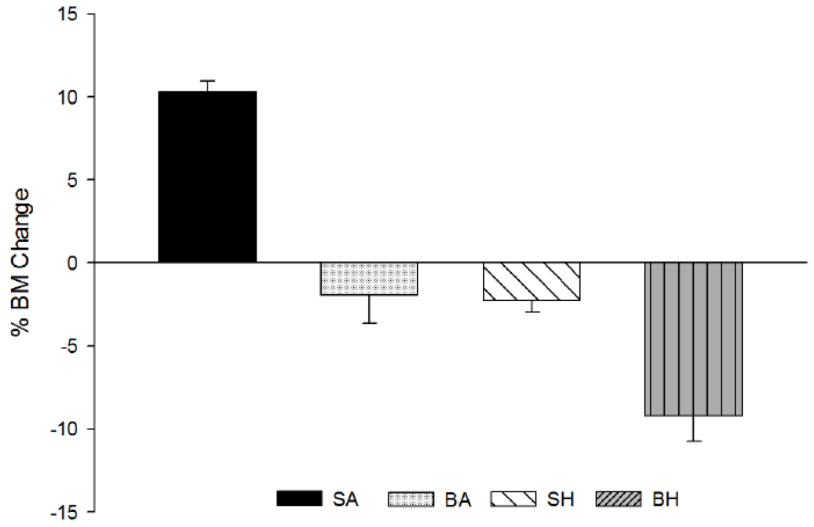

Figure 1.

Percent body mass change from day 0 until day 14 after injury. A significant decrease was observed in all groups as compared to Sham/Ambulatory (SA) ($p<0.05$). Burn/Hindlimb Unloaded (BH) was significantly reduced from Burn/Ambulatory (BA) and Sham/Hindlimb Unloaded (SH) ($p<0.05$).

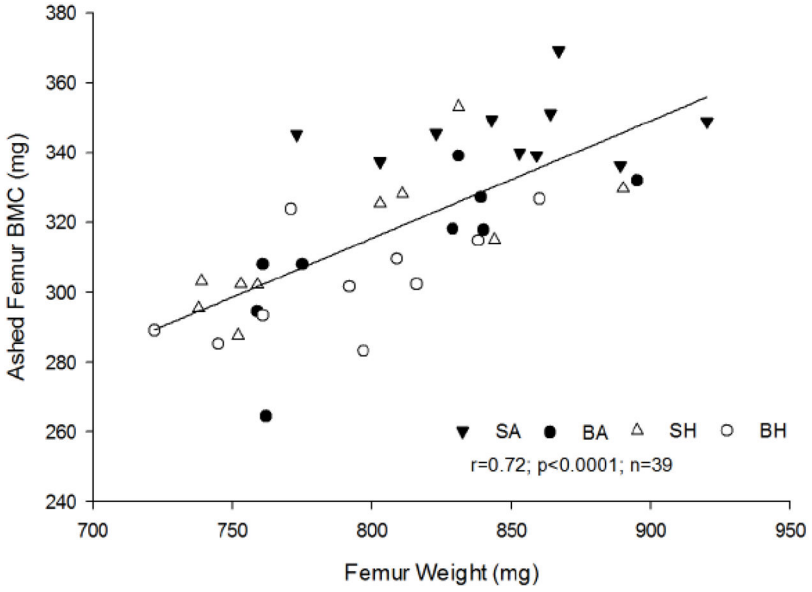

Figure 2.

Relationship between ashed femur bone mineral content (BMC) and femur weight. A positive association was observed, r=0.72; p<0.001, n=39.

Figure 3a

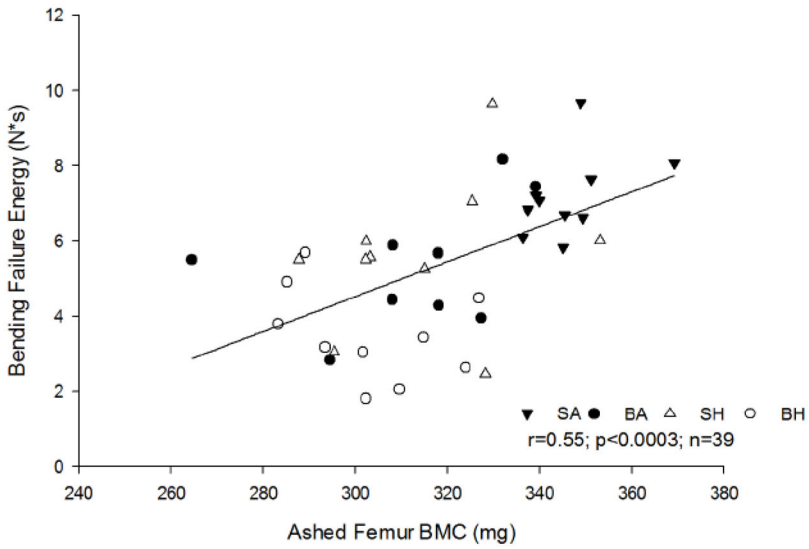

Figure 3b

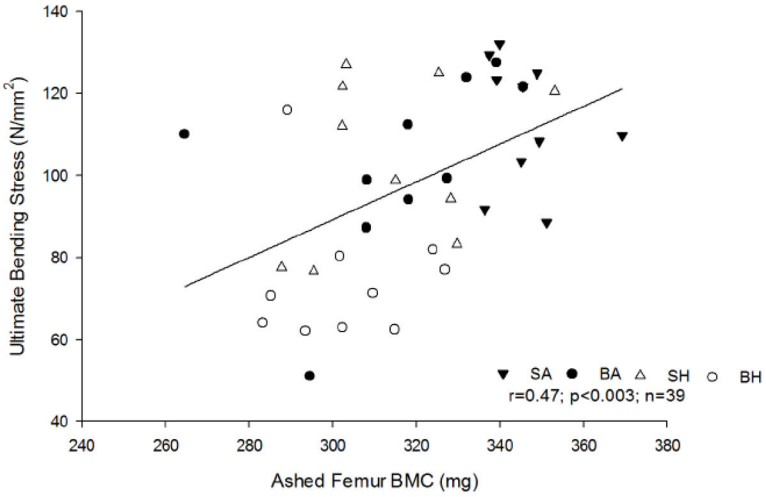

Figure 3.

Figure 3a. Relationship between femur bending failure and ashed femur bone mineral content (BMC). A positive association was observed, r=0.55; p<0.0003, n=39.

Figure 3b. Relationship between ultimate bending stress and ashed femur BMC. A positive association was observed, r=0.47; p<0.003, n=39.

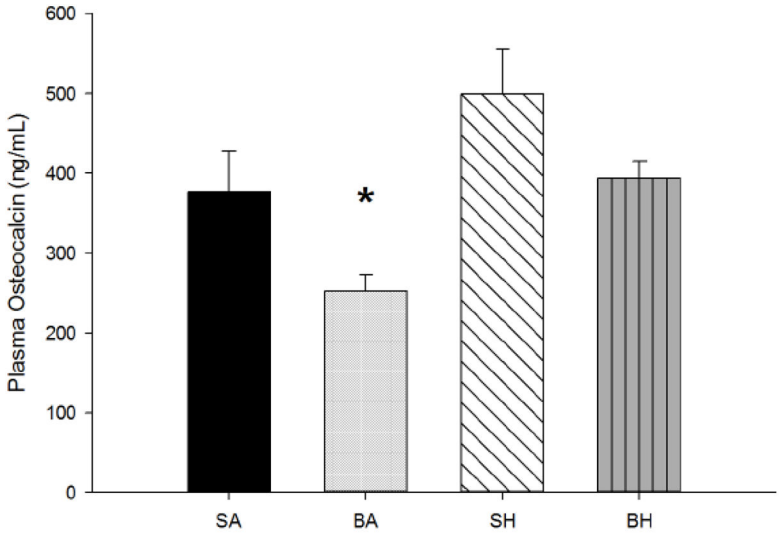

Figure 4.

Mean plasma osteocalcin. Burn/Ambulatory (BA) was significantly reduced as compared to all other treatment groups ($p<0.005$).

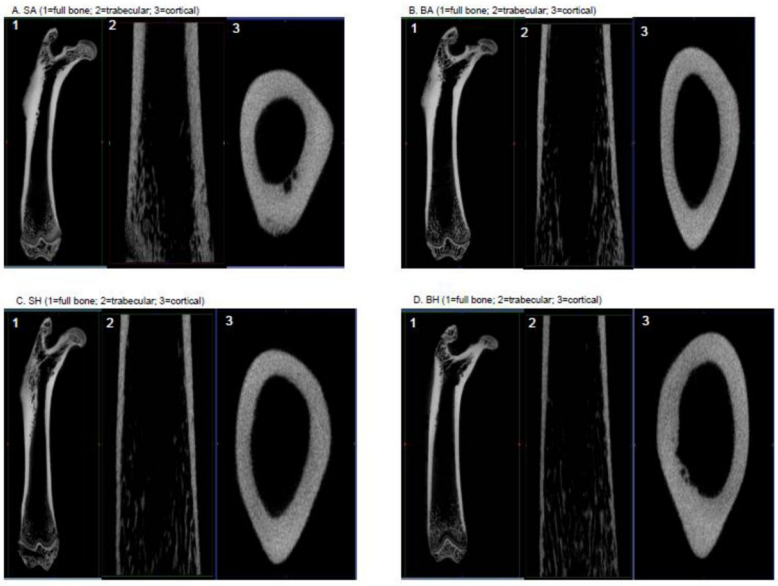

Figure 5.

Figure 5a–d. 3D representations of full femur bone (top L) and 2D representations of cortical (top R) and trabecular (btm R) from Sham/Ambulatory (SA) (a), Burn/Ambulatory (BA) (b), Sham/Hindlimb Unloaded (SH) (c) and Burn/Hindlimb Unloaded (BH) (d).

Table 1

Mean body mass, femur weight, length, diameter, width and ashed femur BMC.

	SA	BA	SH	BH
Body Mass (g)-Day 0	298±3	304±1	306±2	303±2
Body Mass (g)-Day 14	335±6	301±2[a]	299±4[a]	277±12[a]
Femur Wt (g)	0.85±0.01	0.81±0.02	0.79±0.02[a]	0.79±0.01[a]
Femur Length (mm)	36.3±0.1	36.1±0.2	35.8±0.2	35.6±0.1[a]
Femur Length (mm)	3.36±0.04	3.34±0.05	3.22±0.05	3.31±0.05
Femur Length (mm)	3.92±0.07	3.84±0.37	3.75±0.07	3.89±0.05
Ashed Femur BMC (mg)	346.2±3.1	312.2±7.1[a]	314.2±6.6[a]	302.9±4.9[a]

[a] significantly different from SA ($p<0.005$)

SA=Sham/Ambulatory; BA=Burn/Ambulatory; SH=Sham/Hindlimb Unloaded; BH=Burn/Hindlimb Unloaded

Table 2

Femur bone mechanical properties.

	SA	BA	SH	BH
Peak Force (N)	141.2±2.8	119.0±6.8	116.0±5.5	92.3±5.5
Bending Failure Energy (N*s)	7.2±0.4	5.4±0.5[a]	5.6±0.7[a]	3.5±0.4[a]
Ultimate Stiffness (N/mm)	1368±60	1485±49	1435±150	1457±92
Ultimate Bending Stress (N/mm^2)	113.3±4.9	99.8±8.3	104.3±6.8	75.4±5.2[a,b,c]
Young's Modulus (N/mm^2)	673.4±64.7	628.7±63.4	716.9±80.6	450.8±50.5[a,c]

[a] significantly different from SA ($p<0.005$);

[b] significantly different from BA ($p<0.005$)

[c] significantly different from SH ($p<0.005$)

SA=Sham/Ambulatory; BA=Burn/Ambulatory; SH=Sham/Hindlimb Unloaded; BH=Burn/Hindlimb Unloaded

Table 3

Mean daily intake, plasma, urinary and ashed femur minerals.

	SA	BA	SH	BH
Daily Ca^{++} Intake (mg/day)	200±3	190±4	180±3	180±5
Daily P Intake (mg/day)	1.4±0.03	1.4±0.03	1.3±0.02	1.3±0.04
Plasma Ca^{++} (mg/dL)	9.5±0.2	9.5±0.2	9.3±0.1	9.7±0.3
Plasma P (mg/dL)	84±0.2	9.7±0.7	8.8±0.3	8.9±0.3
Urinary Ca^{++} (mg/day)	150.7±14.7	182.8±19.8	159.6±12.3	178.9±15.1
Urinary P (mg/day)	326.8±38.0	554.7±49.8[a]	428.1±50.2	687.7±70.7[a,b]
Ashed Ca^{++} (mg/g bone)	2729.1±144.12	2577.35±162.52	2653.66±125.04	2584.21±93.35
Ashed P (mg/g bone)	1286.87±58.99	1238.84±69.06	1273.13±40.34	1243.01±42.16

[a] significantly different from SA ($p<0.005$);

[b] significantly different from SH ($p<0.005$)

Table 4

Femur bone uCT properties.

Full Bone	SA	BA	SH	BH
Vol (mm^3)	647±15	590±20[a,d]	604±17[a,d]	544±15[a]
BMC (mg)	474±16	434±19[a]	455±22	401±16[a,c]
BMD (mg/cc)	730±9	733±9	751±15	736±8
TMC (mg)	461±16	422±19[a]	442±21	390±15[a,c]
TMD (mg/cc)	753±10	758±11	780±16	760±9
BVF	0.94±0.001	0.94±0.001	0.94±0.001	0.94±0.001

Midshaft Cortical	SA	BA	SH	BH
Mean Thickness (mm)	0.88±0.01	0.82±0.02[a]	0.85±0.01	0.81±0.01[a]
Inner Perimeter (mm)	8.42±0.15	8.7±0.2	8.4±0.14	8.8±0.2
Outer Perimeter (mm)	14.5±0.23	14.3±0.16	14.0±0.2	14.2±0.2
Marrow Area (mm^2)	5.27±0.19	5.68±0.27	5.21±0.2	5.7±0.2
Cortical Area(mm^2)	9.42±0.12	9.0±0.13[a]	8.9±0.2	8.8±0.1[a]
Total Area (mm^2)	14.7±0.22	14.7±0.24	14.2±0.2	14.5±0.2
Midshaft BMD (mg/cc)	937±15.4	946.7±19.8	971.1±24.5	936±16.6
Midshaft BMC (mg)	0.22±0.01	0.19±0.01	0.22±0.01	0.21±0.01
Ct.Ar/Tt.Ar	0.64±0.01	0.55±0.01	0.63±0.01	0.61±0.01

Distal Trabecular	SA	BA	SH	BH
Total Volume (mm^3)	61.6±1.9	69.8±2.3	69.1±2.4	70.0±2.8[a]
Euler Number	709.8±175	412.1±194	777.2±184	572.9±115.5
Connectivity Density (1/mm^3)	8.0±2.3	5.3±2.2	8.9±2.3	8.4±2.0
BV/TV	0.14±0.01[b]	0.12±0.02[b]	0.19±0.02	0.14±0.02[b]
BS/BV	37.9±1.7[b]	39.2±0.8[b]	33.1±1.3	42.1±1.7[b]
Tb.Th.	0.05±0.001	0.05±0.001	0.06±0.001	0.05±0.001
Tb.N	2.6±0.2	2.3±0.3	3.1±0.2	2.8±0.3
Tb.Sp.	0.34±0.02	0.44±0.07	0.28±0.03	0.35±0.04
BMD (mg/cc)	169.5±15.9[b]	162.2±9.9[b]	218.8±16.2	184.4±14.2

[a] significantly different from SA ($p<0.005$);

[b] significantly different from BA ($p<0.005$);

[c] significantly different from SH ($p<0.005$);

[d] significantly different from BH ($p<0.005$)

[a] significantly different from SA ($p<0.005$);

[b] significantly different from BA ($p<0.005$);

[c] significantly different from SH ($p<0.005$);

[d] significantly different from BH (p<0.005)

[a] significantly different from SA (p<0.005);

[b] significantly different from SH (p<0.005)

SA=Sham/Ambulatory; BA=Burn/Ambulatory; SH=Sham/Hindlimb Unloaded; BH=Burn/Hindlimb Unloaded